Conformational analysis, NMR properties and nitrogen inversion of N-substituted 1,3-oxazines†

Marcela Hurtado,[a] J. Guillermo Contreras,*[a] Adelio Matamala,[a] Otilia Mó[b] and Manuel Yáñez*[b]

Received (in Montpellier, France) 28th May 2008, Accepted 9th July 2008
First published as an Advance Article on the web 3rd September 2008
DOI: 10.1039/b808929a

The conformational preference of a set of selected N-substituted oxazines has been investigated at the MP2/6-311 + G(d,p) and B3LYP/6-311 + G(d,p) levels of theory. From the ΔG^0 calculated values, it can be concluded that when the substituent is methyl, ethyl and propyl the axial conformation is preferred in the gas phase. When the substituent is isopropyl or *tert*-butyl the equatorial conformer is the most abundant in the gas phase. This situation does not change in solution provided the solvent has very low polarity as Cl_4C, in good agreement with the experimental findings. However, when the polarity of the solvent increases, the stabilization of the equatorial conformer is quite significant, due to its large dipole moment, and it becomes the dominant form in $CHCl_3$ and CH_2Cl_2 solvents. Quite importantly, the percentage of axial conformer obtained from the values of the ^{1}H chemical shift are in good agreement with the percentage obtained from the calculated free energy. The nitrogen inversion barrier of N-substituted 1,3-oxazines decreases with the size of the substituent. The largest substituent stabilizes the nitrogen lone-pair to the greatest extent in the transition state and is the one that least interacts with the ring when it becomes planar.

1. Introduction

The oxazines are cyclic compounds generated from the substitution of two atoms of carbon in the cyclohexane, for a nitrogen atom and one of oxygen. These substitutions distort the chair conformation which is commonly observed as the most stable structure in cyclohexane and related derivatives.

Since the 1950s oxazinic derivatives have attracted the attention of researchers for two reasons, their pharmacological activity,[1,2] and their reactivity and molecular structure.[3,4] Examples of its powerful biological activity are given in the works by Urbanski *et al.*[1a] and Eckstein *et al.*,[1b] which gave evidence for the cytotoxic activity and antitumor properties of 5-nitrotetrahydro-1,3-oxazine derivatives. Other examples are the antileukemic antibiotics macrolides such as Maytansine, Maytanprine and Maytanbutine with tetrahydro-1,3-oxazine-2-one structures,[2] and *Maytenus ovatus*, *Maytenus buchananii* and *Maytenus serrata* studied by Meyers *et al.*[1c] From the structural point of view these derivatives represent a convenient example to study both the conformational effect of introducing heteroatoms into the ring and the preferred orientation of the alkyl group attached to nitrogen in the heterocycle. For this reason, the 1,3-oxazines have been studied and a considerable amount of experimental data on these compounds already exists.[3] Among the first studies is the work done by Urbanski *et al.*[4a] who concluded that this type of heterocycles exhibit a chair conformation and that the nitro group is preferred in the axial position. Eliel and co-workers[4b] confirmed this observation. Allingham *et al.*[3d] through a NMR analysis extended previous studies[4a] to the *n*-propyl, isopropyl and cyclohexyl derivatives. The ^{1}H NMR data allowed determining the preferential conformation by studying the J_{gem} for C2, C4 and C6 protons. These coupling constants would be sensitive to orientation of the nitrogen lone-pair, and showed that methyl, ethyl and propyl substituents must exist predominantly in axial conformation whereas isopropyl and *tert*-butyl substituents are predominantly in equatorial conformation. Factors such as electronic delocalization, electrostatic repulsions and steric factors, are the predominant ones dictating the most stable nitrogen conformation.[5]

Few papers have reported the percentage of a given conformer in the chemical equilibrium of 1,3-oxazines. Katritzky and co-workers[6] found that ΔG°_{138} is *ca.* −0.16 kcal mol^{-1} for the equatorial–axial equilibrium in 3-methyl-1-oxa-3-aza-cyclohexane, the dominant component being that having an axial methyl group. Also, Lehn and Riddell[3e] measured the axial–equatorial free energy differences for N-methyl in tetrahydro-1,3-oxazines series. The aim of this work is to show that ^{1}H chemical shifts can be used to determine the percentage (α) of each conformer in the chemical equilibrium. For this purpose we shall use the experimental chemical shift measured

[a] *Facultad de Ciencias Químicas, Universidad de Concepción, casilla 160-C Concepción, Chile*
[b] *Departamento de Química, C-9, Universidad Autónoma de Madrid, Cantoblanco, 28049 Madrid, Spain.*
E-mail: gcontrer@udec.cl; manuel.yanez@uam.es

† Electronic supplementary information (ESI) available: Table S1: B3LYP/6-31G** optimized geometries for N-substituted oxazines. Table S2: Total energies (E), zero point energy corrections (ZPE), enthalpy thermal corrections (H_{corr}), Gibb's free energy thermal corrections (G_{corr}), entropy (S), dipole moments (μ), relative enthalpies (ΔH°) and relative Gibb's free energies (ΔG°) for isomers. Table S3: Relative free energies of the axial isomer of the methyl and ethyl derivatives obtained at two different levels of theory. See DOI: 10.1039/b808929a

by Allingham *et al.*[3d] to determine the α parameter which will be compared with that obtained from the theoretical calculation of free energy assuming a Boltzmann distribution.

We have considered also interesting to calculate the nitrogen inversion barrier for each of the compounds included in this study, since it seems well established that for multiheteroatom six-membered rings the ring inversion barrier is higher than the nitrogen inversion barrier, provided the heteroatoms are not adjacent.[7] Very few works[3f,6,8] regarding the nitrogen inversion barrier in oxazinic rings, have been reported in the literature. In this respect is worth mentioning the work of Lehn *et al.*,[3f] in which the nitrogen inversion barrier on non-nitrate oxazines was investigated by means of variable-temperature NMR techniques.

2. Computational methods

Standard *ab initio* and density functional theory (DFT) calculations were performed using GAUSSIAN 03 series of programs.[9] The geometry optimization of all conformers was carried out with a 6-31G(d,p) basis set at HF[10] and B3LYP[11] level. Frequency calculations were carried out to assess that all the found structures were local minima or transition states. The energy calculations were carried out using 6-31G(d,p), 6-311G(d,p), 6-311 + G(d,p) and 6-311 + + G(d,p) basis sets in order to observe the effect of including both polarization and diffuse functions as well as electron correlation at the second-order Møller–Plesset[12] theory and B3LYP. The calculated energies were corrected with the zero-point vibrational energies (ZPE) and thermal corrections were also taken into account to calculate the free energies.

The solute–solvent interactions were accounting for by using Tomasi's Polarizable Continuum Model (PCM)[13] at both the MP2/6-311 + G(d,p)//HF/6-31G(d,p) and B3LYP/6-311 + G(d,p)//B3LYP/6-31G(d,p) levels of theory, which will be named as MP2/A and BLYP/B, hereafter. The following solvents: tetrachloromethane, CCl_4 ($\varepsilon = 2.2379$), chloroform ($\varepsilon = 4.8069$) and dichloromethane ($\varepsilon = 8.93$)[14] were considered, and a temperature of 298.0 K was employed. Besides the electrostatic terms which are well described in this method, the non-electrostatic ones, mainly due to cavitation and dispersion may be also important as their relative contribution may significantly modify values. The dispersion contribution is calculated using the Floris and Tomasi approximation[15] whereas the cavitation term[16] is obtained assuming that the solute is composed of spherical atoms of radii R_i equal to the van der Waals radii multiplied by scale of 1.21. The surface of each sphere is subdivided in 70 tesserae. Although the treatment of non-electrostatic terms is a weakness of these models, it should have a small effect in our analysis, where the contribution of these terms should not be dramatically different for the two isomers, at least for polar solvents.

The equilibrium standard free energy in a solvent ($\Delta G^0_{solution}$) is given by:

$$\Delta G^0_{solution} = \Delta G^0_{gas} + \Delta\Delta G^0_{solvation} \quad (1)$$

where ΔG^0_{gas} is the gas free energy change and $\Delta\Delta G^0_{solvation}$ corresponds to the change in the free energy of solvation, which includes the polarization contributions and non-electrostatic terms such as cavitation, dispersion and repulsion energies. The solvation free energy is regarded as the difference between the free energy in solution and the free energy in gas phase.

The percentage (α) of each conformer in the chemical equilibrium is calculated according to the relationship:

$$\Delta G^0 = -RT\ln K \quad (2)$$

where

$$K = \alpha/(1-\alpha) \quad (3)$$

To obtain the theoretical ^{1}H chemical shifts (δ), the B3LYP/6-31G(d,p) optimized geometries were used for the compounds under study and for tetramethylsilane (TMS), which was used as standard. The magnetic shielding tensors were calculated at B3LYP/6-311 + G(d,p)//B3LYP/6-31G(d,p) level of theory using the Gauge-Independent Atomic Orbital (GIAO) method.[17] Chemical shifts were derived with respect to the NMR isotropic magnetic shielding tensors (in ppm) from the corresponding standard tensors (TMS = 31.904 ppm for ^{1}H).

The percentage of each conformer in the chemical equilibrium can be alternatively estimated from the ^{1}H chemical shifts through the relationship:

$$\delta^{=}_{calc,i} = (1-\alpha)\delta^0_{eq,i} + \alpha\delta^0_{ax,i} \quad (4)$$

where, $\delta^0_{eq,i}$ and $\delta^0_{ax,i}$, are the chemical shifts of nucleus i in the equatorial and axial pure conformer, respectively, and $\delta^{=}_{calc,i}$, corresponds to calculated chemical shifts for the equatorial–axial mixture. The final value of α is calculated by a least squares fitting of λ:

$$\lambda = (\delta^{=}_{exp} - \delta^{=}_{calc})^2_i \quad (5)$$

In order to study the electronic structures of the conformers, Natural Bond Orbital (NBO)[18] analyses were carried out on the B3LYP/6-31G(d,p) geometries and the energies of hyperconjugation interactions, the Fock (F_{ij}) matrix element corresponding to the orbital interactions and the energies of the donor and acceptor orbitals, derived. The hyperconjugation interaction energies were obtained from the second-order perturbation approach: $\Delta E^{(2)}_{\sigma\sigma^*} = -2\langle\sigma|F|\sigma^*\rangle^2/(\varepsilon_{\sigma^*} - \varepsilon_\sigma)$, where the integral corresponds to the F_{ij} matrix element between interacting orbitals i and j whose energies are ε_σ and ε_{σ^*}. The factor 2 stands for the population of the donor orbital. There is a good linear correlation between the second-order perturbation hyperconjugative energies and the deletion procedure.[19] The energy of the hypothetical Lewis molecule with strictly localized bonds is obtained by removing all off-diagonal elements from the Fock matrix and computing one SCF cycle. The information is useful in order to determine the delocalization energy: $E_{deloc} = E_{total} - E_{Lewis}$.

3. Results and discussion

3.1 Molecular structures

The group of oxazines included in this work is formed by 1,3-oxazines substituted in C5 with a nitro group and methyl group, whereas R on N3, can be methyl, ethyl, propyl,

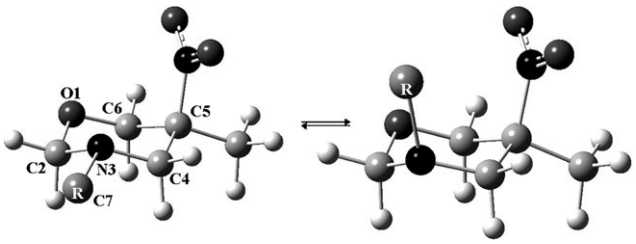

Fig. 1 Equatorial–axial chemical equilibrium in N-substituted oxazines (R = Me, Et, Pr, *i*-Pr, *t*-Bu).

isopropyl or *tert*-butyl group, either axial or equatorial with respect to the nitro group. For oxazines of this type a negligible barrier for the ring inversion has been determined,[3c,4a] and the most abundant structure is that in which the nitro group is in the axial position. Although in principle the nitro group could move to an equatorial position by ring inversion, this process is restricted by the presence of a methyl group at position 5.[3c] Furthermore, different studies[3d,g,4a] on oxazines which are methyl substituted at position 5, indicate that the nitro group is always in the axial position. Hence, only conformers with the nitro group in the axial position (see Fig. 1) have been considered in our study. The numbering used for these systems is shown in Fig. 1.

The optimized geometries for the compounds included in this study are given in Table S1 of ESI.† The structural differences between conformers can be analyzed in terms of the two main effects expected in systems of this kind, the anomeric effect (AE) and the *trans* lone-pair effect. According to the AE[20] (see Fig. 2), the stabilization of axial conformation is due to the overlap between nitrogen lone-pair and the σ^*_{CX} orbital, where X is an electron-withdrawing group.

Therefore, according to Fig. 2, the anomeric effect is responsible for the axial structures having longer O1C2 and C5C4 bond distances, and shorter C2N3 and N3C4 bond distances with respect to the standard value C–N (1.47 Å). This effect also accounts for the opening of the O1C2N3 and C5C4N3 angles. However, in order to reduce the destabilizing diaxial interactions between the N-substituent and NO_2 present on C5, the angle C5C4N3 opens to some extent.

The *trans* lone-pair effect results from an interaction between the N lone-pair and the σ^*_{CH} antibonding orbital. Such stereoelectronic interactions are only possible in the equatorial

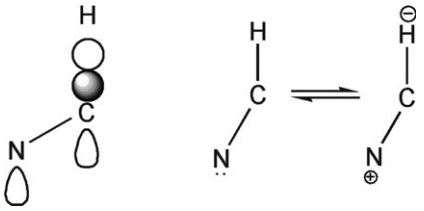

Fig. 3 *Trans* lone-pair effect.

conformation and are responsible for these structures having long C2H2a and C4H4a distances, and also short C2N3 and N3C4 distances.

The *trans* lone-pair effect has been also observed in amines[21] in which the bond C–H is orientated antiperiplanar to the lone pair of nitrogen (see Fig. 3). The above mentioned amines show a C–H stretching frequency related to a weakening of the bond. A similar effect is also found in compounds that have oxygen instead of nitrogen, but the effect is less intense due to the larger electronegativity of the oxygen atom. This *trans* lone-pair effect results in a widening of the H2aC2N3 and H4aC4N3 angles in the equatorial conformers. This effect is reflected in red-shifting of the C2–H and C4–H stretching frequencies on going from the axial to the equatorial conformer, which for the N-methyl substituted derivative are 142 and 129 cm^{-1}, respectively.

Both, the equatorial and axial conformers, show a significant difference between the C2O1C6C5 and C2N3C4C5 dihedral angles; this difference being larger for the axial conformer. These dihedral angles can be taken as a measure of the degree of distortion of the ideal chair conformation in the cyclohexane, where both dihedral angles are the same in absolute value. The difference observed in the oxazines studied here comes from the distortion produced by the two different heteroatoms (O and N) in the ring. This difference is larger the bulkier are the substituents on N. Also in both axial and equatorial conformers the O1C2N3 angle is larger than the C4C5C6 angle. This effect is again larger in the axial conformer and increases with the size of the substituent. The above angles are also sensitive to the magnitude of the diaxial interactions between the NO_2 and R groups across the ring (see Fig. 4(a)), which forces them to move away one from each other. As a consequence of the O1C2N3 bond angle being larger, the repulsive interaction between the heteroatoms

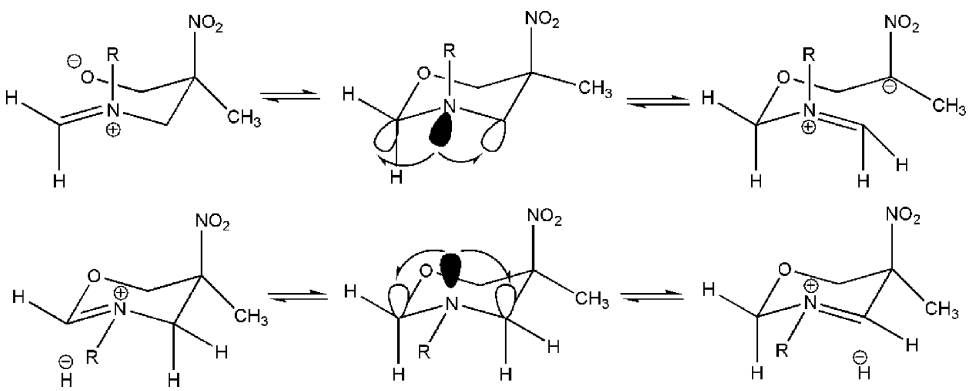

Fig. 2 Interactions related to the anomeric and *trans* lone-pair effects.

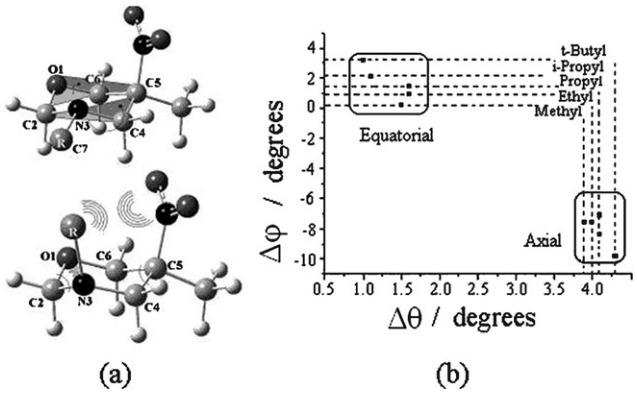

Fig. 4 (a) Diaxial interactions in the axial conformer and (b) Dieterich–Paul–Curtin diagram showing the correlation between the difference in the C2O1C6C5 and C2N3C4C5 dihedral angles ($\Delta\varphi$) and differences in the O1C2N3 and C4C5C6 bond angles ($\Delta\theta$).

would become smaller. The most important conclusion of this analysis is that these geometrical parameters allow to easily discriminate between axial and equatorial conformers through the use of a diagram similar to that of Dieterich–Paul–Curtin[22] in which the differences between the C2O1C6C5 and C2N3C4C5 dihedral angles are plotted *vs.* the differences between the O1C2N3 and C4C5C6 bond angles. As is clearly shown in Fig. 4(b), equatorial and axial conformers are grouped in opposite corners of the diagram.

3.2 Relative stabilities

The total energies, zero point energy corrections, enthalpy and free energy corrections, obtained at different levels of theory are summarized in Table S2 of ESI.† It is worth noting that the inclusion of a second set of diffuse functions on the H atoms, leads to a negligible change in the calculated relative energies, while the computational time is four times larger. A good agreement between MP2/6-311+G(d,p) and B3LYP/6-311+G(d,p) levels of theory is observed and the latter will be adopted throughout the paper. The calculated relative enthalpies and free energies, taking the equatorial conformer as reference, are given in Table 1. This table includes also the dipole moment of each species.

From Table 1, it can be inferred, that both theoretical models, based on MP2 or B3LYP energies predict the axial conformer to be slightly more stable than the equatorial at least for the methyl, ethyl and propyl substituents, whereas for isopropyl and *tert*-butyl a reverse situation is found. For the particular case of the methyl substituent, both conformers are predicted to be close in energy, but while the MP2 method predicts the axial conformer to be slightly more stable than the equatorial one, the opposite prediction derives from B3LYP calculations. Interestingly, the NMR studies in CCl_4

Table 1 Dipole moment (μ, Debye), relative enthalpy (ΔH^0_{298}) and relative Gibbs free energy (ΔG^0_{298}) in kcal mol^{-1} for N-substituted oxazines

		Methyl		Ethyl		Propyl		Isopropyl		*tert*-Butyl	
Model		Ax.	Eq.	Ax.	Eq.	Ax.	Eq.	Ax.	Eq.	Ax.	Eq.
MP2/A	μ	4.160	5.578	4.129	5.483	4.130	5.411	4.149	5.368	4.119	5.272
	ΔH^0_{298}	−0.47	0.0	−4.96	0.0	−1.10	0.0	0.20	0.0	0.32	0.0
	ΔG^0_{298}	−0.29	0.0	−2.18	0.0	−0.67	0.0	0.61	0.0	1.30	0.0
B3LYP/B	μ	3.528	4.736	3.496	4.654	3.478	4.598	3.498	4.616	3.472	4.527
	ΔH^0_{298}	0.24	0.0	−0.42	0.0	−0.42	0.0	0.79	0.0	0.97	0.0
	ΔG^0_{298}	0.43	0.0	−0.08	0.0	0.07	0.0	1.17	0.0	1.77	0.0

Table 2 Calculated relative Gibbs free energy in solution ($\Delta G^0_{solution}$, kcal mol^{-1}) for the axial conformer of N-substituted oxazines. The percentage of the axial conformer is given in parentheses

Solvent	Theoretical model	Methyl	Ethyl	Propyl	Isopropyl	*tert*-Butyl
Gas	MP2/A	−0.29	−0.44	−0.67	0.61	1.29
		(62.0)	(67.8)	(75.8)	(26.3)	(10.1)
	B3LYP/B	0.43	−0.08	0.07	1.17	1.77
		(32.5)	(53.2)	(47.1)	(12.2)	(4.8)
CCl_4	MP2/A	−0.04	0.68	−0.21	0.87	1.24
		(51.7)	(53.0)	(59.0)	(18.7)	(10.9)
	B3LYP/B	0.50	0.13	0.38	1.33	1.55
		(29.9)	(44.4)	(34.6)	(9.6)	(6.8)
$CHCl_3$	MP2/A	0.42	0.40	0.26	1.38	1.76
		(33.0)	(33.7)	(39.4)	(8.9)	(4.9)
	B3LYP/B	0.83	0.48	0.71	1.67	1.93
		(19.7)	(30.6)	(23.2)	(5.6)	(3.7)
CH_2Cl_2	MP2/A	0.68	0.68	0.48	1.64	1.64
		(24.1)	(24.1)	(30.6)	(5.9)	(5.9)
	B3LYP/B	1.01	0.68	0.89	1.87	2.12
		(15.3)	(23.9)	(18.2)	(4.1)	(2.7)

conducted by Allingham and Cookson[3d] concluded that for methyl, ethyl and propyl substituents the preferred conformer is the axial one, whereas the equatorial structure is the predominant one when the substituent is isopropyl and *tert*-butyl. These relative stabilities change slightly when the interaction with the solvent is included using the PCM approach[13] (see Table 2). The smallest changes are observed, as expected, for apolar CCl_4. In this case the relative stability of the axial isomer in solution is larger than the equatorial one. For methyl, ethyl and propyl substituents axial preference is derived, whereas for isopropyl and *tert*-butyl substituents the equatorial form becomes the most stable, in good agreement with the experimental findings.[3d]

Substantial changes are observed however when the other two solvents are considered. In fact, the equatorial conformer becomes systematically the most stable form. This decrease in the presence of the axial conformer as the dielectric constant of the solvent increases is presented in Fig. 5, and is a clear consequence of the increase in the dipole moment of the system (See Table 1). The main conclusion of this theoretical work is that neither in the gas phase nor in solution the N-substituted 1,3-oxazines will ever be found as conformationally pure compounds, but as mixtures of axial and equatorial conformers. The axial conformer will be dominant in the gas-phase and in non-polar solvents for small substituents such as methyl, ethyl or propyl. However, the larger dipole moment of the equatorial conformers will stabilize them in moderate polar solvents, and this form becomes the dominant one in these media, independently of the size of the substituent.

It is worth noting that for the *tert*-butyl derivative the curve presents a small maximum when the solvent is Cl_4C. This is may be due to a poor performance of the PCM model for this apolar solvent, for which dispersion will be a significant contribution to the solvation energy.

Since the energy difference between the two conformers is rather small, the errors in their estimated abundances can be significant, and may depend on the accuracy of the theoretical model. In order to have an idea of the reliability of our analysis we have re-calculated the relative stabilities of the axial and equatorial conformers of the methyl and ethyl

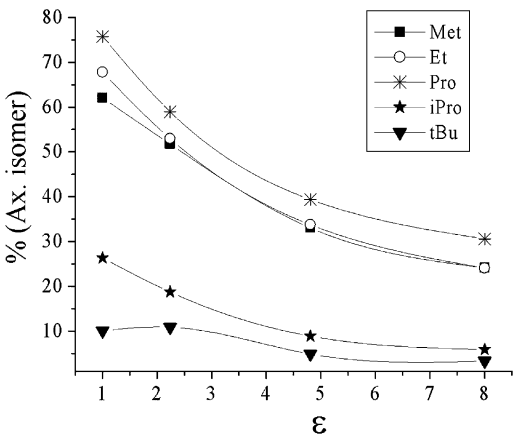

Fig. 5 Variation of the percentage of axial isomer present in solution as a function of the dielectric constant, ε, of the solvent.

Table 3 MP2/A calculated ^{1}H chemical shifts (ppm) and B3LYP/B calculated J_{HH} coupling constants (Hz) for N-substituted oxazines (G = gas phase, S = solution, E = experimental value)

	Methyl					Ethyl					Propyl					Isopropyl					*tert*-Butyl				
	Ax.		Eq.			Ax.		Eq.			Ax.		Eq.			Ax.		Eq.			Ax.		Eq.		
	G	S	G	S	E	G	S	G	S	E	G	S	G	S	E	G	S	G	S	E	G	S	G	S	E
H2a	4.32	4.38	3.43	3.5	3.96	4.15	4.21	3.32	3.39	4.03	4.12	4.18	3.39	3.45	4.02	4.14	4.19	4.12	4.17	4.05	4.21	4.26	3.8	3.86	4.03
H2e	4.39	4.39	4.3	4.3	4.08	4.6	4.6	4.56	4.55	4.19	4.55	4.55	4.54	4.54	4.18	4.6	4.6	4.28	4.29	4.25	4.87	4.86	4.71	4.71	4.35
H6a	3.37	3.47	3.12	3.22	3.57	3.37	3.46	3.14	3.24	3.56	3.39	3.48	3.12	3.22	3.56	3.38	3.48	3.19	3.28	3.53	3.34	3.43	3.16	3.25	3.48
H6e	5.12	5.1	4.94	4.91	4.41	5.08	5.06	4.95	4.93	4.44	5.09	5.07	4.93	4.91	4.44	5.13	5.1	4.93	4.9	4.36	5.02	5	4.92	4.89	4.32
H4a	3.04	3.13	1.94	2.06	2.77	3.19	3.27	2.09	2.2	2.82	3.14	3.23	2.12	2.23	2.81	3.23	3.31	2.26	2.36	2.75	2.98	3.06	2.3	2.4	2.7
H4e	4.15	4.14	3.91	3.91	3.47	4.16	4.16	3.87	3.87	3.59	4.16	4.16	3.86	3.86	3.6	4.21	4.21	4	4	3.54	4.48	4.47	4.2	4.2	3.58
J_{2e2a}	−10.1		−7.2		−8.6	−10.5		−7.3		−9	−10.4		−7.2		−8.8	−10.9		−7.3		−8	−11		−7.5		−7.7
J_{6e6a}	−11.7		−11.3		−12	−11.6		−11.3		−12	−11.6		−11.3		−12	−11.6		−11.2		−12	−11.6		−11.2		−12
J_{4a4a}	−13.8		−10.9		−13	−13.8		−10.9		−13.2	−13.8		−10.8		−13.4	−14.2		−10.9		−12.4	−14.4		−10.8		−12
J_{4e6e}	2.5		2.1		2	2.5		2.1		2	2.5		2.1		2	2.4		2		2	2.3		1.9		
J_{2e4e}	1.4		1		1.1	1.5		1.1		1.2	1.5		1.1		1.2	1.8		1.4		1.2	1.9		1.6		

derivatives by significantly enlarging the basis set. This assessment was done for both the gas-phase and the most polar solvent. As shown in Table S3 of ESI,† small changes are observed in the energy differences as well as on the estimated abundances when the basis set is enlarged, but these changes are too small to affect our conclusions, in the sense that in the gas-phase the axial conformer is still the dominant one, while the equatorial one is the most abundant in CH_2Cl_2 solutions.

3.3 NMR parameters

The calculated ^{1}H-NMR chemical shifts are summarized in Table 3, along with the corresponding experimental values. Calculated J_{HH} coupling constants are also included in this table.

It is obvious from our previous discussion that the experimental available data should correspond to equatorial/axial mixtures, where the two conformers contribute to the experimental chemical shift (δ) as a function of their relative abundance.

Therefore, following the methodology proposed at the beginning of this work, the calculated chemical shift is obtained using eqn (4). As a suitable example we present in Fig. 6(a) the least square fitting of the parameter α for the N-methyl substituent. Fig. 6(b) shows the reasonably good correlation between the experimental and the calculated chemical shifts when α is set to minimize the error. The five substituents show similar behavior and the corresponding correlations between experimental and calculated ^{1}H chemical shifts are summarized in Table 4.

Once the value of α is obtained for each substituent it is possible to calculate the percentage of each conformer by means of eqn (4). The percentage of axial conformer obtained by this method in CCl_4, is comparable to that obtained from the calculated free energies assuming a Boltzmann distribution (see Table 5). The results obtained with both approaches, indicate that for the methyl substituent an almost equal proportion of the two conformers is present, whereas for ethyl and propyl the axial isomer is slightly dominant. The situation changes completely for the substituents isopropyl and *tert*-butyl, for which the equatorial conformer is the preferred one in good agreement with the experimental results. For *tert*-butyl, the relative concentration of equatorial conformer in solution is as large as 96.8%, that compares only approximately with the value derived from the NMR data (89.2%), likely due, as indicated above, to the difficulty associated with the correct treatment of the dispersion contributions within the PCM model when the solvent is CCl_4 and the substituent is bulky.

Table 4 Linear regression between calculated and experimental chemical shifts

N-Substituent	Correlation	R^2
Methyl	$\delta_{calc} = 1.35\delta_{exp} - 1.13$	0.87
Ethyl	$\delta_{calc} = 1.29\delta_{exp} - 0.92$	0.86
Propyl	$\delta_{calc} = 1.29\delta_{exp} - 0.95$	0.87
Isopropyl	$\delta_{calc} = 1.33\delta_{exp} - 1.11$	0.90
tert-Butyl	$\delta_{calc} = 1.38\delta_{exp} - 1.27$	0.87

3.4 Nitrogen inversion barriers

The nitrogen inversion barriers both in terms of energies and free energies calculated for the N-substituted oxazines included in this study are given in Table 6.

Table 5 Relative abundance (%) of the axial conformer in CCl_4 solution derived from calculated free energies (MP2/A) and ^{1}H NMR (B3LYP/B) using eqn (4)

N-Substituent	MP2/A	B3LYP/B
Methyl	51.7	49.9
Ethyl	53.0	55.6
Propyl	59.0	54.0
Isopropyl	18.7	17.9
tert-Butyl	10.9	3.2

Table 6 Nitrogen inversion barriers (kcal mol^{-1}) relative to the most stable conformer

Substituent	ΔE^a	ΔG
Methyl	3.6^b	3.8^b
Ethyl	2.9^b	3.2^b
Propyl	2.6^b	3.0^b
Isopropyl	2.3^c	2.9^c
tert-Butyl	1.4^c	2.4^c

^{a} These values include the ZPE correction. ^{b} Values relative to the axial conformer. ^{c} Values relative to the equatorial conformer.

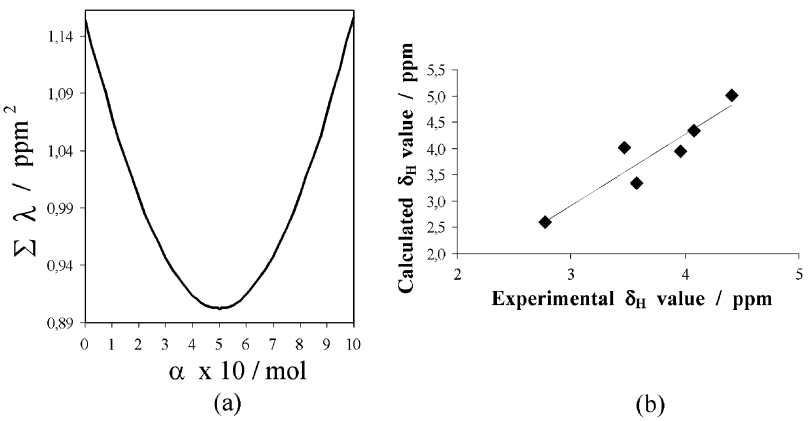

Fig. 6 (a) Least-square fitting of the parameter α for the N-methyl substituent. (b) Correlation between calculated and experimental ^{1}H chemical shifts, using for the latter the value of α obtained in Fig. 6(a). The correlation obeys the relation $\delta_{calc} = 1.35\delta_{exp} - 1.13$; $R^2 = 0.87$.

From this table it can be concluded that the barrier decreases with the number of methylene or methyl groups in the substituent, the smallest being those of the isopropyl and *tert*-butyl derivatives. The decrease in the inversion barrier of nitrogen with the increase in the size of the substituent could be analyzed in a similar form to that carried out in amines and amides.[23] Two factors may be responsible for the stabilization of the transition state when the size of the substituent increases: its ability to stabilize the electron lone-pair and its ability to stabilize the substituent.

It is known that the nitrogen changes its hybridization along the inversion process from sp^3 in any of the local minima to sp^2 in the transition state, where the lone-pair occupies a pure p orbital.[24] These hybridization changes are clearly reflected in the corresponding NBO analysis (see Table 7).

Since the nitrogen lone-pair has a p character in the planar transition state it would be stabilized by electron-deficient adjacent carbons. An inspection of the natural charges of the three carbon atoms directly linked to nitrogen, namely C2, C4 and C7, reveal that the electron population of the former two remains practically constant (around 5.932 and 6.274, respectively) when changing the substituent. Conversely, the natural electron population of C7, the carbon of the substituent directly bonded to nitrogen, decreases steadily following the trend (methyl (6.465) < ethyl (6.248) < propyl (6.247) < isopropyl (6.045) < *tert*-butyl (5.846)) reflecting the markedly different inductive effects of the substituents considered. This trend is clearly in agreement with that observed for the N inversion barriers. The second factor behind the low barrier calculated for the *tert*-butyl derivative reflects the difference in the destabilization of the transition state produced by the substituent through an electron transfer towards the nitrogen. The greater is the s character of the N orbital in its planar form, the stronger is this interaction which causes a net destabilization of the transition state. An examination of the N–C7 distances along the series (methyl (1.444 Å) < ethyl (1.454 Å) < propyl (1.454 Å) < isopropyl (1.465 Å) < *tert*-butyl (1.485 Å)) clearly indicates that the s character, and accordingly the interaction, are the smallest for the *tert*-butyl derivative, again in agreement with its low N inversion barrier.

We have considered it of interest to compute the energy profile along the inversion process, following the intrinsic reaction coordinate for the methyl and ethyl substituents. The results are presented in Fig. 7(a) and (b), respectively. When the substituent is methyl, only a typical inversion barrier that links the axial with the equatorial conformation is found. When the substituent is an ethyl group, two transition states are observed, reflecting a certain coupling between the N

Table 7 Contribution of the atomic orbitals (%) to the lone-pair of electrons of the nitrogen

		Eq.			TS			Ax.		
Substituent	ν_{im}[a]/cm^{-1}	s	p	d	s	p	d	s	p	d
Methyl	152.50i	14.9	85.0	0.1	0.2	99.8	0.0	12.7	87.2	0.1
Ethyl	95.26i	15.0	85.0	0.0	0.7	99.3	0.0	12.4	87.6	0.0
Propyl	73.36i	14.7	85.2	0.0	0.7	99.3	0.0	12.0	88.0	0.0
Isopropyl	78.17i	14.7	85.2	0.0	0.1	99.9	0.0	12.1	87.9	0.0
tert-Butyl	79.96i	11.5	88.4	0.0	0.6	99.4	0.0	6.4	93.6	0.0

[a] Calculated at the B3LYP/B level.

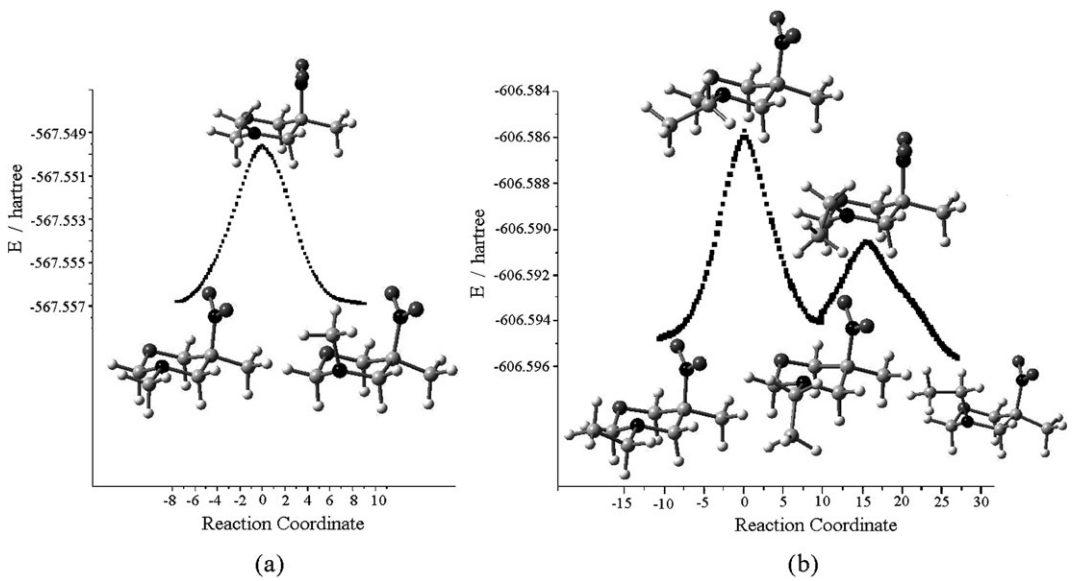

Fig. 7 Energy profiles for the nitrogen inversion process in (a) 5-nitro-3,5-dimethyl-1,3-oxazine and (b) 5-nitro-5-methyl-3-ethyl-1,3-oxazine.

inversion and the internal rotation of the substituent. The dominant contribution to the first barrier comes from the inversion process, although a slight rotation of the substituent is also observed. The second activation barrier is essentially associated to internal rotation of the substituent group, as reflected in the corresponding imaginary frequency of 136.8 cm^{-1}.

In this respect it is worth mentioning that this coupling between rotation and inversion was reported for ethylamine barriers by During and Li[25] and Fisceher and Botskor[26] using Raman and microwave spectroscopic techniques.

4. Conclusions

From the results outlined above some interesting conclusions can be drawn:

1. From the ΔG^0 calculated values we were able to determine the conformational preference in a set of selected oxazines. It can be concluded that when the substituent is methyl, ethyl and propyl the axial conformation is the preferred one in the gas-phase. When the substituent is isopropyl or *tert*-butyl the equatorial conformer is the most abundant. This situation does not change in solution provided the solvent has very low polarity such as CCl_4, in good agreement with the experimental findings. However, when the polarity of the solvent increases, the stabilization of the equatorial conformer is quite significant due to its large dipole moment, and it becomes the dominant species in $CHCl_3$ and CH_2Cl_2 solvents.

2. The percentage of axial conformer obtained from the values of the ^1H chemical shift are in good agreement with the percentage derived from free energies, except for *tert*-butyl substituent likely due to the difficulty associated with the correct treatment of the dispersion contributions within the PCM model.

3. The distance N3–C7, the dihedral angles that conform the ring (C2N3C4C5 and C2O1C6C5) and the O1C2N3 and C4C5C6 bond angles, are the structural parameters most sensitive to the N-substituent effect. Quite interestingly, the correlation between the difference in the values of the aforementioned dihedral angles and the difference in the values of the O1C2N3 and C4C5C6 bond angles, allow to clearly discriminate between axial and equatorial conformers.

4. Likewise to amines and amides, the nitrogen inversion barrier of N-substituted 1,3-oxazines decreases with the size of the substituent. The largest substituent stabilizes the most the nitrogen lone-pair in the transition state and is the one that least interacts with the ring when it becomes planar. Some coupling between the nitrogen inversion and the internal rotation of the substituent is observed for the ethyl substituent, and would very likely also exist in larger substituents as propyl.

Acknowledgements

This work was partially supported by an operating grant (No 203,021.019-1.0) from the Universidad de Concepcion, Chile. S. M. H. O thanks CONICYT for a scholarship.

References

1 (*a*) T. Urbanski, D. Gürne, S. Slopek, H. Mordaska and M. Mordarski, *Nature*, 1960, **187**, 426–427; (*b*) Z. Eckstein, P. Gluzinski, E. Grochowski, M. Mordarski and T. Urbanski, *Bull. Acad. Pol. Sci., Ser. Sci. Chim.*, 1962, **10**, 331; (*c*) A. I. Meyers, C. C. Shaw, D. Horne, L. M. Trefonas and R. J. Majeste, *Tetrahedron Lett.*, 1975, **16**, 1745–1748.
2 (*a*) S. M. Kupchan, Y. Komoda, W. A. Court, G. J. Thomas, R. M. Smith, A. Karim, C. J. Gilmore, R. C. Haltiwanger and R. F. Bryan, *J. Chem. Soc., Chem. Commun.*, 1972, 1065; (*b*) S. M. Kupchan, Y. Komoda, W. A. Court, G. J. Thomas, R. M. Smith, A. Karim, C. J. Gilmore, R. C. Haltiwanger and R. F. Bryan, *J. Am. Chem. Soc.*, 1972, **94**, 1354–1356.
3 (*a*) T. Urbanski, *Nature*, 1951, **168**, 562–563; (*b*) T. Urbanski, C. Z. Radzikowski, Z. Ledóchowski and W. Czarnocki, *Nature*, 1956, **178**, 1351–1352; (*c*) T. Urbanski, *Synthesis*, 1974, **9**, 613–632; (*d*) Y. Allingham, R. C. Cookson, T. A. Crabb and S. Vary, *Tetrahedron*, 1968, **24**, 4625–4630; (*e*) F. G. Riddell and J. M. Lehn, *J. Chem. Soc. B*, 1968, **10**, 1224–1228; (*f*) J. M. Lehn, Pierre Linscheid and F. G. Riddell, *Bull. Soc. Chim. Fr.*, 1968, **3**, 1172–1177; (*g*) D. Gürne, T. Urbanski, L. Stefaniak and M. Witanowski, *Tetrahedron, Suppl.*, 1963, **6**, 211–218.
4 (*a*) D. Gürne and T. Urbanski, *J. Chem. Soc.*, 1959, 1912–1913; (*b*) M. K. Kaloustian, N. Dennis, S. Mager, S. A. Evans, F. Alcudia and E. L. Eliel, *J. Am. Chem. Soc.*, 1976, **98**, 956–965.
5 Guillermo Contreras, Marcia M. C. Ferreira, S. Marcela Hurtado, Lorena A. Gerli and R. Pilar Castillo, *J. Chil. Chem. Soc.*, 2005, **50**, 731–737.
6 I. J. Ferguson, A. R. Katritzky and D. M. Read, *J. Chem. Soc., Perkin Trans. 2*, 1980, 1739–1745.
7 (*a*) R. K. Harris and R. A. Spragg, *J. Chem. Soc. B*, 1968, 684–691; (*b*) J. E. Anderson, *J. Am. Chem. Soc.*, 1969, **91**, 6374–6380.
8 (*a*) I. J. Ferguson, A. R. Katritzky and D. M. Read, *J. Chem. Soc., Chem. Commun.*, 1975, 255–256; (*b*) I. J. Ferguson, A. R. Katritzky and D. M. Read, *J. Chem. Soc., Perkin Trans. 2*, 1977, 818–820.
9 M. J. Frisch, G. W. Trucks, H. B. Schlegel, G. E. Scuseria, M. A. Robb, J. R. Cheeseman, J. A. Montgomery, Jr., T. Vreven, K. N. Kudin, J. C. Burant, J. M. Millam, S. S. Iyengar, J. Tomasi, V. Barone, B. Mennucci, M. Cossi, G. Scalmani, N. Rega, G. A. Petersson, H. Nakatsuji, M. Hada, M. Ehara, K. Toyota, R. Fukuda, J. Hasegawa, M. Ishida, T. Nakajima, Y. Honda, O. Kitao, H. Nakai, M. Klene, X. Li, J. E. Knox, H. P. Hratchian, J. B. Cross, V. Bakken, C. Adamo, J. Jaramillo, R. Gomperts, R. E. Stratmann, O. Yazyev, A. J. Austin, R. Cammi, C. Pomelli, J. Ochterski, P. Y. Ayala, K. Morokuma, G. A. Voth, P. Salvador, J. J. Dannenberg, V. G. Zakrzewski, S. Dapprich, A. D. Daniels, M. C. Strain, O. Farkas, D. K. Malick, A. D. Rabuck, K. Raghavachari, J. B. Foresman, J. V. Ortiz, Q. Cui, A. G. Baboul, S. Clifford, J. Cioslowski, B. B. Stefanov, G. Liu, A. Liashenko, P. Piskorz, I. Komaromi, R. L. Martin, D. J. Fox, T. Keith, M. A. Al-Laham, C. Y. Peng, A. Nanayakkara, M. Challacombe, P. M. W. Gill, B. G. Johnson, W. Chen, M. W. Wong, C. Gonzalez and J. A. Pople, *GAUSSIAN 03 (Revision D.01)*, Gaussian, Inc., Wallingford, CT, 2004.
10 (*a*) A. Szabo and N. S. Otslund, *Modern Quantum Chemistry*, MacGraw-Hill, New York, 1989; (*b*) W. J. Hehre, L. Radom, P. V. Schleyer and J. A. Pople, *Ab initio Molecular Orbital Theory*, Wiley-Interscience, New York, 1986.
11 (*a*) A. D. Becke, *Phys. Rev. A*, 1988, **38**, 3098–3100; (*b*) S. H. Vosko, L. Wilk and M. Nusair, *Can. J. Chem.*, 1980, **58**, 1200–1211; (*c*) C. Lee, W. Yang and R. G. Parr, *Phys. Rev. B*, 1988, **37**, 785–789.
12 M. Head-Gordon, J. A. Pople and M. Frisch, *Chem. Phys. Lett.*, 1988, **153**, 503–506.
13 (*a*) S. Miertus, E. Scrocco and J. Tomasi, *Chem. Phys.*, 1981, **55**, 117–129; (*b*) J. Tomasi, R. Bonaccorsi, R. Cammi and F. J. Olivares del Valle, *J. Mol. Struct. (THEOCHEM)*, 1991, **234**, 401–424.
14 Ch. Wohlfarth, *Static Dielectric Constants of Pure Liquids and Binary Liquid Mixtures*, Springer-Verlag, Berlin and New York, 1991, vol. IV/6.

15 (*a*) F. M. Floris, A. Tani and J. Tomasi, *Chem. Phys*., 1993, **169**, 11–20; (*b*) F. M. Floris and J. L. P Ahuir, *J. Comput. Chem*., 1991, **12**, 784–791; (*c*) F. M. Floris and J. Tomasi, *J. Comput. Chem*., 1989, **10**, 616–627.
16 (*a*) R. A. Pierotti, *Chem. Rev*., 1976, **76**, 717–726; (*b*) J. Langlet, P. Claverie, J. Caillet and A. Pullman, *J. Phys. Chem*., 1988, **92**, 1617–1631.
17 (*a*) J. R. Chesseman, G. W. Trucks, T. A. Keith and M. J. Frisch, *J. Chem. Phys*., 1996, **104**, 5497–5509; (*b*) J. Foresman and A. Frisch, *Exploring Chemistry with Electronic Structure Methods: A Guide to using Gaussian*, Gaussian Inc., Pittsburgh, PA, 1996.
18 E. D. Glendening, J. K. Badenhoop, A. E. Reed, J. E. Carpenter, J. A. Bohmann, C. M. Morales and F. Weinhold, *NBO 5.G*, Theoretical Chemistry Institute, University of Wisconsin Madison, WI, 2004.
19 I. V. Alabugin and T. A. Zeidan, *J. Am. Chem. Soc*., 2002, **124**, 3175–3185.
20 (*a*) R. V. Lemieux, *Pure Appl. Chem*., 1971, **25**, 527–548; (*b*) *Anomeric Effects: Origin and Consequences ACS. Symp. Ser. 87*, ed. W. A. Szarek and D. Horton, American Chemical Society, Washington, DC, 1979; (*c*) A. J. Kirby, *The Anomeric Effect and Related Stereoelectronic Effects at Oxygen*, Springer-Verlag, Berlin, 1983; (*d*) M. L. Sinot, *Adv. Phys. Org. Chem*., 1988, **24**, 113; (*e*) E. Juaristi and G. Cuevas, *The Anomeric Effect*, CRC Press, Boca Raton, FL, 1995.
21 H. D. Thomas, K. Chen and N. L. Allinger, *J. Am. Chem. Soc*., 1994, **116**, 5887–5897.
22 (*a*) D. A. Dieterich, Iain C. Paul and D. Curtin, *J. Am. Chem. Soc*., 1974, **96**(20), 6372–6380; (*b*) A. L. Llamas-Saiz, C. Foces-Foces and J. Elguero, *J. Mol. Struct*., 1994, **319**, 231–260; (*c*) O. Mó, M. Yáñez, A. L. Llamas-Saiz, C. Foces-Foces and J. Elguero, *Tetrahedron*, 1995, **51**, 7045–7062.
23 (*a*) K. B. Wiberg and C. Breneman, *J. Am. Chem. Soc*., 1992, **114**, 831–840; (*b*) A. D. Bain, P. Hazendonk and P. Couture, *Can. J. Chem*., 1999, **77**, 1340–1348; (*c*) K. E. Laiding and L. M. Cameron, *Can. J. Chem*., 1993, **71**, 872–879; (*d*) K. E. Laiding and L. M. Cameron, *J. Am. Chem. Soc*., 1996, **118**, 1737–1742.
24 C. L. Perrin, J. D. Thoburn and S. Elsheimer, *J. Org. Chem*., 1991, **56**, 7034–7038.
25 J. R. During and Y. S. Li, *J. Chem. Phys*., 1975, **63**, 4110–4113.
26 (*a*) E. Fisceher and I. Botskor, *J. Mol. Spectrosc*., 1982, **91**, 116–127; (*b*) E. Fisceher and I. Botskor, *J. Mol. Spectrosc*., 1984, **104**, 226–247; (*c*) E. Fisceher and I. Botskor, *J. Mol. Struct*., 1983, **97**, 93–96.